Received: 10 March 2022 | Revised: 30 August 2022 | Accepted: 19 September 2022

DOI: 10.1002/jex2.64

RESEARCH ARTICLE

Integrins are enriched on aberrantly fucosylated tumour-derived urinary extracellular vesicles

Md. Khirul Islam[1,2] | **Bert Dhondt**[3,4,5] | **Parvez Syed**[6] | **Misba Khan**[1] | **Kamlesh Gidwani**[1] | **Jason Webber**[7] | **An Hendrix**[4,5] | **Guido Jenster**[8] | **Tarja Lamminen**[9] | **Peter J. Boström**[9] | **Kim Pettersson**[1] | **Urpo Lamminmäki**[1,2] | **Janne Leivo**[1,2]

[1]Department of Life Technologies, Division of Biotechnology, University of Turku, Turku, Finland

[2]InFLAMES Research Flagship Center, University of Turku, Turku, Finland

[3]Department of Urology, Ghent University Hospital, Ghent, Belgium

[4]Laboratory for Experimental Cancer Research, Department of Human Structure and Repair, Ghent University, Ghent, Belgium

[5]Cancer Research Institute, Ghent University, Ghent, Belgium

[6]Inme Inc., Turku, Finland

[7]Institute of Life Science 1, Swansea University Medical School, Swansea, UK

[8]Department of Urology, Erasmus MC, Rotterdam, The Netherlands

[9]Department of Urology, Turku University Hospital and University of Turku, Turku, Finland

Correspondence
Janne Leivo, Molecular Biotechnology and Diagnostics, Department of Life Technologies, University of Turku, Kiinamyllynkatu 10, FI-20014 Turku, Finland.
Email: jpleiv@utu.fi

Abstract

Urinary extracellular vesicles (uEVs) are enriched with glycosylated proteins which have been extensively studied as putative biomarkers of urological cancers. Here, we characterized the glycosylation and integrin profile of EVs derived from urological cancer cell lines. We used fluorescent europium-doped nanoparticles coated with lectins and antibodies to identify a biomarker combination consisting of integrin subunit alpha 3 (ITGA3) and fucose. In addition, we used the same cancer cell line-derived EVs as analytical standards to assess the sensitivity of the ITGA3-UEA assay. The clinical performance of the ITGA3-UEA assay was analysed using urine samples of various urological pathologies including diagnostically challenging benign prostatic hyperplasia (BPH), prostate cancer (PCa) and bladder cancer (BlCa). The assay can significantly discriminate BlCa from all other patient groups: PCa (9.2-fold; $p = 0.00038$), BPH (5.5-fold; $p = 0.004$) and healthy individuals (and 23-fold; $p = 0.0001$). Our results demonstrate that aberrantly fucosylated uEVs and integrin ITGA3 can be detected with fucose-specific lectin UEA in a simple bioaffinity assay for the detection of BlCa directly from unprocessed urine.

KEYWORDS
Bladder cancer, Extracellular vesicle, Glycosylation, Immunoassay, Integrin, Lectin, Nanoparticle, Prostate cancer, Prostate cancer

1 | INTRODUCTION

Urological cancers, primarily cancers of the prostate and bladder, are a significant cause of morbidity and mortality worldwide (Ferlay et al., 2015; Siegel et al., 2018; Siegel et al., 2013). The majority of currently available diagnostic modalities for the detection of prostate cancer (PCa) lack sufficient clinical specificity for accurate diagnosis. Whilst there have been major advances in multiparametric magnetic resonance imaging (mp-MRI) technique there remains a degree of ambiguity, thus necessitating the need for biopsy (Ahmed et al., 2017). Although non-invasive methods which reduce mortality are widely used, including measurement of circulating prostate specific antigen (PSA), limitations resulting from overdiagnosis makes the cancer specificity of the assay questionable. Equal socio-economic burden derives from bladder cancer (BlCa), the ninth most common type of cancer (Ferlay et al., 2015; Raitanen et al., 2001; Siegel et al., 2017). Currently, cystoscopy and urine cytology is considered the gold standard for BlCa detection. Cystoscopy is an effective but invasive test for BlCa detection. Moreover, it has a low sensitivity for carcinoma in situ (Tis) (Raitanen et al., 2001). On the other hand, cytology is a non-invasive test, but it has low sensitivity for low-grade tumours (Lotan & Roehrborn, 2003). Non-invasive urine-based biomarkers have been studied and approved by the Food and Drug Administration (FDA), such as bladder tumour antigen (BTA), nuclear matrix protein 22 (NMP22) and ImmunoCyt+ test. Despite the FDA approval, none of these markers have demonstrated satisfactory potential to be used in daily practice (Charpentier et al., 2021; Chou et al., 2015; Oeyen et al., 2019; Smith & Guzzo, 2013). Although enormous scientific and clinical efforts have been made, the need for simple and specific diagnostic tools for the non-invasive detection of urological cancers persists.

The use of extracellular vesicles (EVs) as cancer biomarkers has received unprecedented interest in the past decade. EVs can be detected directly from biological fluids, including blood and urine, providing easily accessible biomarkers for early diagnostics (Shephard et al., 2021) and disease monitoring (Ma et al., 2019; Zhou et al., 2020). The analysis of the biomolecular composition of the EV cargo by sampling biological fluids has led to the identification of exceptionally disease-specific biomarkers (Zhang et al., 2019). Despite this promise, the biomolecular complexity, and the sheer number of different secreted EV subtypes have made the clinical validation of the found biomarkers extremely challenging, particularly from biofluids. The biomolecules encapsulated within EVs contain a myriad of different proteins, nucleic acids and carbohydrates. This is important for cancer diagnosis as the cancer cells release higher amounts of EVs compared to the normal cells (Pang et al., 2020). Others and we have shown that EVs are highly enriched in tetraspanins (CD9, CD63, CD81) and other transmembrane proteins found abundantly in various types of vesicles (Andreu & Yanez-Mo, 2014; Duijvesz et al., 2015; Islam et al., 2019; Raposo & Stoorvogel, 2013). In addition to disease diagnostics, tetraspanin-based assays have been applied for the simple quantification of EVs (Islam et al., 2019; Shao et al., 2018). Tetraspanins, often found clustered in webs, or tetraspanin-enriched microdomains (TEMs), throughout the plasma membrane tether various other membrane-bound proteins around them, including integrins. In previous studies, EV integrins have been shown to have a fundamental role in cancer progression and metastasis (Hamidi & Ivaska, 2018; Hurwitz & Meckes, 2019). Integrins, which are multi-functional cell-adhesion molecules play a key role in extracellular matrix attachment and signal transduction, and serve in the pathways of cell growth, proliferation and migration (Hamidi & Ivaska, 2018; Hou et al., 2016; Huttenlocher & Horwitz, 2011). Recently, various studies showed that different integrin sub-units are found on EVs derived from cancer cells (Fedele et al., 2015; Hoshino et al., 2015; Hurwitz et al., 2016; Paolillo & Schinelli, 2017; Rana et al., 2012; Singh et al., 2016).

Glycosylation of proteins and lipids is known to be aberrant during cancer development and progression, making them a lucrative target for cancer diagnosis (Dube & Bertozzi, 2005). The discrimination of benign and malignant cases directly from biofluids was initially achieved with the use of lectins, glycan-binding proteins identified from both exogenous and endogenous sources (Turner, 1992). Several studies have shown that the clinical specificity of cancer biomarkers can be enhanced significantly by detecting the glyco-isoforms of the proteins such as CA-125 (Gidwani et al., 2016; Jankovic & Milutinovic, 2008) and CA-15-3 (Terävä et al., 2019).

In this study, we explored the presence of integrin-associated aberrant glycosylation on cell line- and urine-derived EVs. We used high-performance lectin nanoparticles, capable of detecting different glycosylation profiles for the screening of EVs by anti-integrin antibody-lectin combinations. The most abundantly expressed biomarkers were subsequently identified using EVs derived from PCa and BlCa patient urine samples. The analytical and clinical performance of the ITGA3-UEA assay was ultimately assessed with the use of urine samples containing various urological pathologies. Our data suggest that laminin binding integrin ITGA3 and aberrantly fucosylated glycans are enriched on tumour-derived urinary EVs and could be used for the detection of BlCa directly from unprocessed urine.

2 | MATERIALS AND METHODS

2.1 | Reagents

The following antibodies were used for immunostaining of EV-enriched and protein-enriched urine fractions: anti-Alix (1:1000 (0.10 μg/ml), 2171 S, Cell Signaling Technology, Beverly, MA, USA), anti-TSG101 (1:1000 (0.20 μg/ml), sc-7964, Santa Cruz

Biotechnology, Dallas, Texas, USA), anti-CD9 (1:1000 (0.23 μg/ml), D3H4P, Cell Signalling Technology), anti-Flotillin-1 (1:1000 (0.25 μg/ml), 610820, BD Biosciences, Franklin Lakes, NJ, USA), anti-THP (1:800 (0.25 μg/ml), sc-20631, Santa Cruz Biotechnology), sheep anti-mouse horseradish peroxidase-linked antibody (1:3000 (0.14 μg/ml), NA931 V, GE Healthcare life sciences, Uppsala, Sweden), donkey anti-rabbit horseradish peroxidase-linked antibody (1:4000 (0.05 μg/ml), NA934V, GE Healthcare life sciences).

HEK293 and MCF10A were used as healthy normal cell line from human embryonic kidney and human breast epithelial cells, respectively. Less aggessive (LNCaP and VCaP) and more aggressive (DU145 and PC3) PCa cell lines were used. T24 and J82 were used as highly aggressive BlCa cell lines. All cell lines were purchased from ATCC (Teddington, UK). RPMI-1640 were purchased from Lonza (Belgium) and 10% fetal bovine serum (FBS) was acquired from GIBCO (USA).

Monoclonal antibodies anti-ITGA1 (clone 639508) (catalog # MAB5676), -ITGA2 (clone HAS3) (catalog # MAB1233), -ITGA3 (clone IA3) (catalog # MAB1345), -ITGA5 (clone 612557) (catalog # MAB18642), -ITGA6 (clone MP4F10) (catalog # MAB1350), -ITGAV (clone 273210) (catalog # MAB1219), -ITGAVB3 (clone 23C6) (catalog # MAB3050), -ITGB1 (4B7R) (catalog # MAB1778), -ITGB4 (clone 422325) (catalog # MAB4060) and -CD9 (clone 209306) (catalog # MAB1880) were purchased from R&D systems (Abingdon, UK). Other monoclonal antibodies anti-ITGAM (clone ICRF44) (catalog # 555386), -ITGAX (clone 3.9) (catalog # 565805), -ITGB2 (clone 6.7) (catalog # 555922), -ITGB3 (clone VI-PL2) (catalog # 555752), and -CD63 (clone 556019) (catalog # 556019) were purchased from BD Bioscience (Vantaa, Finland). Other reagents such as 96-well maxisorp plate and streptavidin-coated yellow plates, red assay buffer, and wash buffer were purchased from Kaivogen Oy (Turku, Finland). Europium (Eu^{3+})-doped monodispersed and carboxyl-modified fluoro-max polystyrene nanoparticles (NPs) were purchased from Seradyn (Indianapolis IN, USA). A panel of recombinant human and plant lectins (Table S1) were acquired from R&D Systems (Abingdon, UK) and Vector laboratories (Burlingame, USA), respectively.

2.2 | Urine samples and patient information

This study was carried out with the approval of the University of Turku ethics committee (ETMK Dnro: 3/1801/2013) and in accordance with the regulations and guidelines of the Helsinki Declaration. Patients diagnosed with prostate or bladder cancer were operated at Turku University Hospital (TYKS) in the period of 2013–2018. Urine sample from healthy volunteers ($n = 18$) were collected at the Biotechnology division, University of Turku in 2020.

All participants involved in this study signed a written informed consent. Urine samples from bladder cancer patients ($n = 32$) were collected by catheterization immediately prior to radical cystectomy or transurethral resection of bladder tumour (TURBT). The study cohort included also urine samples of patients with prostate cancer ($n = 32$) collected by catheterization immediately prior to the robotic-assisted laparoscopic prostatectomy (RALP). Similarly, age-matched urine samples from benign prostatic hyperplasia (BPH) patients were collected as controls before transurethral resection of prostate (TURP). Patient characteristics along with histological classification are included in Table 1. No preprocessing of urine such as centrifugation or filtration was performed prior to the storage of sample. However, urine samples were stored at −80°C until further use.

2.3 | Cell culture and EV separation

Cells were maintained in RPMI-1640 and cultured at Integra bioreactor flask (Integra Biosciences Corp, Hudson, USA), supplemented with L-glutamine (2 mM), penicillin (100 U/ml), streptomycin (100μg/ml), and 10% FBS (Mitchell et al., 2008). EVs from FBS were removed by ultracentrifugation at 100,000 × g for 18 h, followed by serial filtration (0.22μm followed by 0.1μm) using vacuFilter units (Millipore). Cell-conditioned media was collected upon reaching the confluency 80%–100%. Cell-conditioned media was subjected to clear cells and cell-debris by serial centrifugation (400 × g for 10 min followed by 2000 × g for 15 min). EVs were isolated from cell conditioned media by floatation within a 30% sucrose/D_2O cushion before ultracentrifugation at 100,000 × g for 75 min at 4°C within a SW-28 rotator (Beckman Coulter) and a subsequent PBS wash (Lamparski et al., 2002; Théry et al., 2006). Pelleted EVs were resuspended in PBS, quantified based on protein using the BCA-protein assay (Pierce/Thermo, Northumberland, UK), and stored at −80°C prior to further analysis.

2.4 | Urinary EV separation

Urinary EV separation was performed as previously described (Dhondt, Geeurickx, et al., 2020; Dhondt, Lumen, et al., 2020). Urine samples (50 ml) were centrifuged for 10 min at 1000 × g and 4°C in accordance with the Eurokup/HKUPP Guidelines. Cell-free urine supernatants were collected (leaving approximately 0.5 cm urine above the cell pellet) and concentrated to 800 μl using a 10 kDa centrifugal filter device (Centricon Plus-70, Merck Millipore, Massachusetts, USA). Solutions of 5%, 10% and 20% iodixanol were made by mixing appropriate amounts of homogenization buffer (0.25 M sucrose, 1 mM EDTA, 10 mM Tris-HCl

TABLE 1 Patient characteristics

Patient characteristics	Bladder cancer ($n = 32$)	Prostate cancer ($n = 32$)	Benign prostatic hyperplasia ($n = 30$)	Healthy ($n = 18$)
Age (years)				
Median (range)	70; (54–70)	66; (52–75)	70; (57–83)	40; (32–69)
Sex, *n* (%)				
Male	30 (93.8%)	32 (100%)	30 (100%)	18 (100%)
Female	2 (6.2%)			
T-category, *n* (%)				
Tx	1 (3.1%)			
TO	9 (28.1%)			
Ta	1 (3.1%)			
Tis	1 (3.1%)			
T1	4 (12.5%)	11 (34.4%)		
T2	4 (12.5%)	14 (43.8%)		
T3	10 (31.3%)	7 (21.9%)		
T4	1 (3.1%)			
NA	1 (3.1%)			
Tumor grade, *n* (%)				
WHO_ISUP 2004 grade[a]				
Low grade	12 (37.5%)			
High grade	16 (50%)			
NA	4 (12.5%)			
Mx		5 (16%)		
M0		27 (84.0%)		
Nodal stage, *n* (%)				
Nx	2 (6.3%)	9 (28.1%)		
N0	18 (58.2%)	21 (65.6%)		
N1	8 (25%)	2 (6.3%)		
> N1	2 (6.3%)			
NA	2 (6.3%)			
Gleason score (GS), *n* (%)				
GS 6		2 (6.3%)		
GS 7		17 (53.1%)		
GS 8		6 (18.8%)		
GS 9&10		7 (21.9%)		
Surgical treatment, *n* (%)				
TURBT	5 (15.6%)			
Radical cystectomy	27 (84.4%)			
RALP		32 (100%)		
TURP			30 (100%)	

Abbreviations: RALP, robotic-assisted laparoscopic prostatectomy; TURBT, transurethral resection of bladder tumour; TURP, transurethral resection of prostate.
[a]Impact of WHO_ISUP 2004 grading on bladder cancer were used (Lokeshwar et al., 2015).

(pH 7.4)) and iodixanol working solution. This working solution was prepared by combining a working solution buffer (0.25 M sucrose, 6 mM EDTA, 60 mM Tris-HCl, pH 7.4) and a stock solution of OptiPrep (60% (w/v) aqueous iodixanol solution, Axis-Shield, Oslo, Norway). The 800 μl concentrated urine sample was resuspended in 3.2 ml working solution, obtaining a 40% iodixanol suspension, and layered on the bottom of a 17 ml Thinwall Polypropylene Tube (Beckman Coulter, Fullerton, CA, USA). A discontinuous bottom up OptiPrep density gradient was prepared by overlaying the urine suspension with 4 ml 20%, 4 ml 10% and 3.5 ml 5% iodixanol solutions, and 1 ml PBS, respectively. The density gradient was centrifuged for 18 h at 100,000

× *g* and 4°C using a SW 32.1 Ti rotor (Beckman Coulter, Fullerton, California, USA). Fractions of 1 ml were collected from the top of the gradient. EV-enriched fractions 9–10 and protein-enriched (PE) fractions 14–16 were pooled, diluted to 16 ml in PBS in a 17 ml Thinwall Polypropylene Tube (Beckman Coulter) and centrifuged for 3 h at 100,000 × *g* and 4°C (SW 32.1 Ti rotor, Beckman Coulter). The resulting pellets were re-suspended in 100 μl PBS and stored at −80°C until further use.

2.5 | Biotinylation of antibodies

Monoclonal anti-integrin and anti-tetraspanin antibodies were biotinylated using a previously described protocol (Islam et al., 2019; Terävä et al., 2019). The pH of the monoclonal antibody solution was adjusted up to 9.8 by adding 0.5 M carbonate buffer. In the final reaction volume, antibody concentration was ~2 mg/ml. The antibodies were incubated with a 40-fold molar excess of biotin isothiocynate for 4 h at room temperature. After incubation, labelled antibodies were separated from unreacted biotin by NAP-5 gel-filtration columns (GE Healthcare, USA) by using TSA buffer (50 mmol/L Tris-HCl, pH 7.75; 150 mmol/L NaCl and 0.5 g/L NaN_3).

2.6 | Coating of europium –nanoparticles (Eu^{3+}-NPs)

The Eu^{3+}-NPs have long-lifetime fluorescence equivalent to ~30,000 Eu^{3+}per particles (Harma et al., 2001). The utility and efficacy of Eu^{3+}-NPs has been described previously (Gidwani et al., 2016; Harma et al., 2001; Soukka et al., 2001; Terävä et al., 2019). Briefly, antibodies and a list of lectins were covalently coupled to activated carboxyl groups present on the Eu^{3+}-NPs. The nanoparticles (10^{12} particles) were suspended in 10 mmol/L phosphate buffer (pH 7.0) and then 10 mmol/L sulfo-NHS (Sigma-Aldrich, USA) and 0.75 mmol/L EDC (Sigma-Aldrich) were used to active the surface of Eu^{3+}-NPs with a 15 min incubation at RT. In the coupling reaction, the concentration of antibodies and lectins was 0.1 mg/ml. Then, antibodies and lectins conjugated on Eu^{3+}-NPs were stored at 4°C in a buffer supplemented with 10 mM Tris-HCl, pH 7.8, 0.01% and sodium azide, 0.1% BSA. Then, the antibodies and lectins conjugated with Eu^{3+}-NPs were again washed and resuspended and stored in same buffer for 2 days for the removal of aggregates. After centrifugation (350 × *g*, 5 min), aggregates-free supernatant of bioconjugated Eu^{3+}-NPs solution were transferred to a new tube and measured the particles concentration comparing with standard particles concentration. The particles were gently vortexed before every use.

2.7 | Immunoassays

The immunoassay principle is displayed in Figure 1. In direct immunoassay (Figure 1a), approximately 5×10^8 particle per μg protein (P/μg) were passively immobilized in each well of maxisorp plate in 30 μl of PBS buffer. After 2-time washes, 2% BSA (from 7.5% BSA in TSA stock) was added as a blocker with PBS buffer (30 μl/well) followed by 2 h incubation at +4°C. After 2-time washes, 2×10^7 of antibody-NPs or 1×10^7 lectin-NPs were applied to detect immobilized EVs in 30 μl/well assay buffer (Kaivogen Oy, Finland). In the sandwich immunoassay (Figure 1b), biotinylated capture antibodies (100 ng/30 μl/well) were immobilized on 96-well streptavidin-coated microtiter plates in 30 μl assay buffer (Kaivogen Oy, Finland) for 1 h at RT. The wells were washed 2-times with wash buffer (Kaivogen Oy, Finland) using DELFIA plate washer (PerkinElmer). As a sample, purified EVs and unprocessed urine were added. In case of isolated EVs, approximately 5×10^8 P/μg were added in each well in 30 μl of assay buffer. In case of urine, 50 μl of unprocessed urine samples (diluted 1:2 in assay buffer) were added in each well. As a blank, fresh cell culture medium and EV-depleted urine were used. EV-stripped urine was produced by passing a pooled urine sample through MWCO 100 kDa Vivaspin 2 column (Sartorius, Germany). After 1 h incubation at RT with slow shaking, the wells were washed for 2-times before the addition of 2×10^7 of antibody-NPs or 1×10^7 lectin-NPs in a final volume of 30 μl. The NPs were incubated for 2 h at RT with slow shaking (40 × *g*). Time-resolved fluorescence (TRF europium at λ_{ex}: 340 nm; λ_{em}: 615 nm) was measured using Victor1420 multilabel counter (PerkinElmer) from the well surface. All measurements were conducted in triplicates.

2.8 | Analytical performance

The limit of detection (LoD) of the ITGA3-ITGA3 and ITGA3-UEA assays were determined with the use of DU145 EVs spiked in healthy urine depleted of EVs. A series of EV particles, 1×10^6, 1×10^7, 1×10^8, 1×10^9, 1×10^{10} and 1×10^{11} EVs/ml, were tested. The blank calibrator was analysed in 60 replicates and the calibrators 1×10^6, 1×10^7, 1×10^8, and 1×10^9 EV/ml were analysed in 20 replicates. The calibrators 1×10^{10}, and 1×10^{11} EV/ml were analysed in 12 and 6 replicates, respectively. The LoD of the assays were determined for ITGA3-ITGA3 and ITGA3-UEA by fitting the data to Sigmoidal and four parameters logistic (4PL)

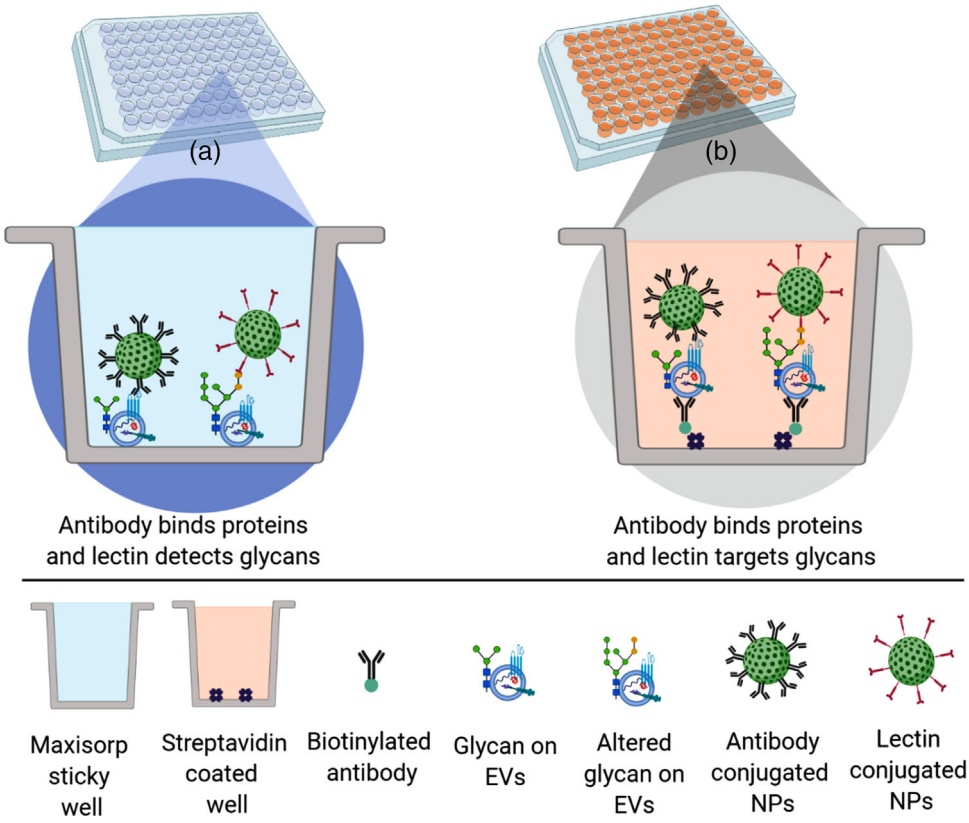

FIGURE 1 Schematic representation of the bioaffinity-assay. (a) Direct assay; EVs were passively immobilised on maxisorp plate and subsequently detected with either antibody or lectin coated nanoparticles (antibody-NPs or lectin-NPs). (b) Sandwich assay; biotinylated antibodies were immobilised on the surface of the streptavidin coated microtiter wells for capturing the EVs. The captured EVs were detected with either antibody or lectin nanoparticles (antibody-NPs or lectin-NPs).

regression of Origin 2016 using the values from standard curves. The LoD was calculated as follows:

$$LoD = \mu_B + 1.645\sigma_B + 1.645\sigma_s$$

where μ_B is the measurement of mean of blank calibrator, σ_B is the measurement of standard deviation of blank and σ_s is the measurement of standard deviation of low concentration calibrators.

2.9 | Nanoparticle tracking analysis

For urinary EVs, nanoparticle tracking analysis (NTA) was performed using a NanoSight LM10-HS microscope (Malvern Instruments Ltd, Amesbury, UK) equipped with a 405 nm laser. For each sample, three 60 s videos were recorded at camera level 13. Temperature was monitored during recording. For cell line derived EVs, NTA was performed using similar NanoSight LM10 system following the previously published article (Webber & Clayton, 2013; Welton et al., 2016) but configured with temperature controlled LM14 laser module with a 488 nm laser. For each sample, three 30 s videos were recorded at camera. Recorded videos were analysed at detection threshold 3 with NTA Software version 3.3 to determine the concentration and size distribution of measured particles with corresponding standard error. A medium viscosity of 0.929 cP was assumed. For optimal measurements, samples were diluted with PBS until particle concentration was within optimal concentration range of the NTA Software (3×10^8–1×10^9). All size distributions determined with NTA correspond to the hydrodynamic diameters of the particles in suspension.

2.10 | Transmission electron microscopy

Urinary EVs were deposited on a formvar-coated grids stabilized with evaporated carbon film and glow discharged before sample application. Neutral uranyl acetate (2% in AD) was used for staining after which grids were coated with 2% methyl

cellulose/uranyl acetate (0.4%) solution. These grids were examined using a Tecnai G2 Spirit transmission electron microscope (FEI, Eindhoven, The Netherlands) operated at 100 kV and images were captured with a Quemesa charge-coupled device camera (Olympus Soft Imaging Solutions GMBH, Munster, Germany) at 9300×, 30,000× and 49,000× magnification. Cell-derived EVs were adsorbed onto formvar-coated grids for 20 min and fixed in 1% (v/v) glutaraldehyde for 5 min. Then grids were washed 3-times in PBS followed by 3-times in distilled water. Grids were then negatively stained with 2% methyl cellulose/uranyl acetate (0.4%) solution for 10 min. These grids were then allowed for air dry before being observed in a JEM-1400 plus TEM (Jeol, Tokyo, Japan) at 80 kV.

2.11 | Western blot

Samples were dissolved in reducing sample buffer (0.5 M Tris-HCl (pH 6.8), 40% glycerol, 9.2% SDS, 3% 2-mercaptoethanol, 0.005% bromophenol blue) and boiled at 95°C for 5 min. Proteins were separated by SDS-polyacrylamide gel electrophoresis and transferred to nitrocellulose membranes (Bio-Rad, Hercules, California, USA). After blocking the membranes, blots were incubated overnight with primary antibodies. Incubation with secondary antibodies was performed after extensive washing of the membranes in PBS containing 0.5% Tween 20. After final washing, chemiluminescence substrate (WesternBright Sirius, Advansta, Menlo Park, California, USA) was added and imaging was performed using Proxima 2850 Imager (IsoGen Life Sciences, De Meern, The Netherlands).

2.12 | Statistical analysis

LoD was calculated using origin 2016 (version 2016Sr2). Statistical analyses using the R software (http://www.r-project.org/), version 3.6.2. Box plots were done with Tidyverse (version 1.3.0) (Wickham et al., Welcome to the tidyverse. J. Open Source Softw. 4, 1686, https://doi.org/10.21105/joss.01686 (2019) and ggpubr (version 0.2.5) R packages (Kassambara, A. ggpubr: 'ggplot2' Based Publication Ready Plots. R package version 0.1. 7. [cited 2020 Jan 08]. Available from: https://CRAN.R-project.org/package=ggpubr). For experiments consisting of two experimental groups statistical significance was assessed using a *t*-test. For experiments consisting of more than two groups we used non-parametric Kruskal-Wallis test where p-value of < 0.05 was considered significant.

2.13 | EV-track

We have submitted all relevant data of our experiments to the EV-TRACK knowledgebase (EV-TRACK ID: EV220092) (Van Deun et al., 2017).

3 | RESULTS

3.1 | Cell line derived EV characterization and quality control

To assess the quality of EVs derived from cancer cells, tetraspanin expression, particle size and morphology of EVs were analysed. The expression of tetraspanins (CD9, CD81 and CD63) was used to confirm the enrichment of EVs from LNCaP, VCaP, PC3 and DU145 using immunofluorescent plate-based assay (Figure 2a). The total number and size of EVs were measured by nanoparticle tracking analysis (NTA) (Figure 2b). The NTA revealed a range of 1.27×10^{13}–1.11×10^{14} EVs particles/ml in purified-EVs samples from PC3, DU145, VCaP and LNCaP cells. Additionally, cell-derived EVs were assessed by transmission electron microscopy (TEM), which showed vesicles surrounded by a lipid bilayer, with an approximate size of 100–200 nm in close-up view (Figure 2c).

3.2 | Characterisation of cell line derived EVs in direct assay

We conducted glycoprofiling of cell line-derived EVs using a series of lectin-NPs which comprise a range of lectins to recognize the most abundantly expressed glycostructures of the human glycome. The lectin-NPs were used as tracers in time-resolved fluorometry-based direct immunoassays to explore the glycan profile of EVs isolated from four PCa-cell lines (LNCaP, VCaP, DU145 and PC3). Altogether 34 lectins (Table S1) with a capacity to recognize six glycans groups, that is, fucose, galactose, GalNAc, GlcNAc, mannose and sialic acid, with different binding specificities were tested. In this initial lectin screening, 12 out

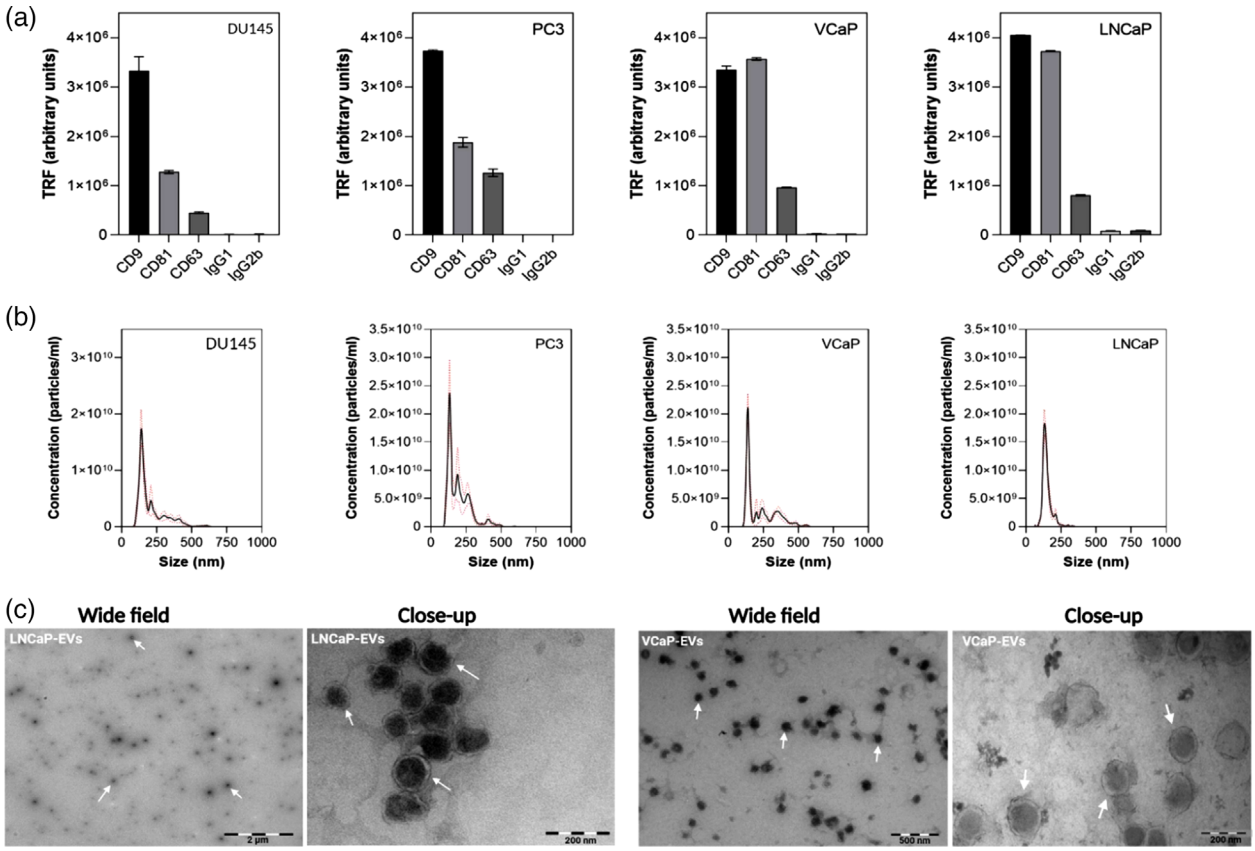

FIGURE 2 Characterisation of EVs-derived from cancer cell lines. The EVs were analysed by (a) tetraspanin expression for CD9, CD81 and CD63 markers and (b) NTA for total number of particles (c) TEM images of isolated EVs. Here, TRF means time-resolved fluorescence. TEM images of LNCaP-EVs and VCaP-EVs were used as a representative image

of the 34 lectins, namely, UEA, TJA-II, SBA, PNA, Galectin-3, WFA, BPL, WGA, PWM, DC-SIGN, ConA and MAA showed strong binding intensities towards EVs (Figure 3a).

We also analysed the expression profile of different integrin sub-units on EVs isolated from the PCa cell lines. Nanoparticles coated with antibodies against 12 different integrin subunits were analysed for their binding to passively coated EVs. As in the case of lectins, clearly distinguishable binding profiles to cancer cell-derived EVs was also observed with anti-integrin antibodies (Figure 3b).

3.3 | Characterisation of cell line derived EVs in sandwich assay

To further analyse the performance of the lectins, we set up a sandwich assay where ITGA3-based capture was used for immobilization of EVs-derived from LNCaP, VCaP, DU145 and PC3. The 12 lectins that showed highest binding intensities in the previous direct assays were then applied for the detection of captured EVs. Among the selected lectins, the fucose-binding lectin UEA clearly showed the highest S/B ratios with all the four-cell line derived EVs (Figure S1).

Next, we explored the capacity of UEA-NPs to recognize various integrins expressing sub-populations of EVs captured from cell culture medium of non-cancer, PCa and BlCa origin (Figure 4). Among the integrin sub-units, ITGA3-based capture resulted in the highest S/B-ratio with EVs from both PCa and BlCa cell lines and showed also the largest difference in S/B-ratio as compared to non-cancer cell-derived EVs (Figure 4).

3.4 | Urine-derived EV characterization and quality control

To investigate urine sample, next, we separated urine from cancer patients by density gradient-enrichment into two fractions such as EV-enriched proteins (fractions 9–10) and non-EV-enriched proteins (fractions 14–16). These urine fractions were characterized by Western blot (WB). WB demonstrated the presence of EV-enriched proteins such as Alix, Flotillin-1, TSG-101, CD9

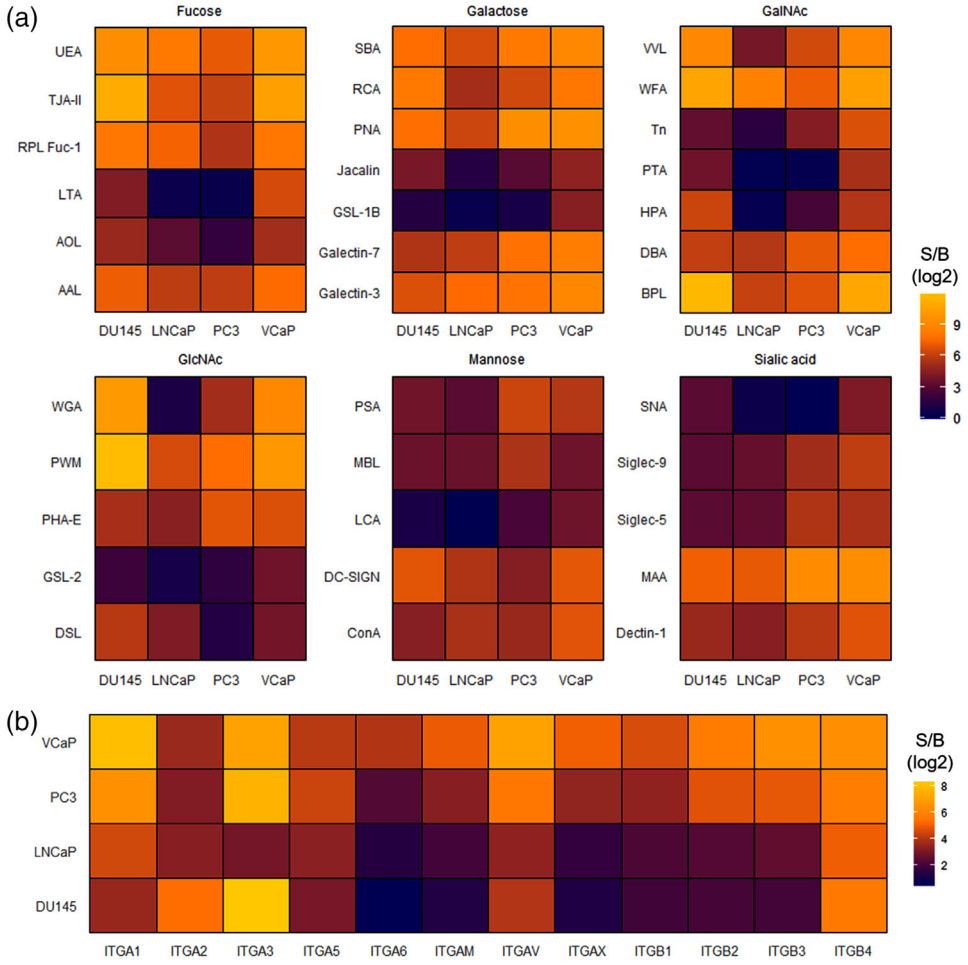

FIGURE 3 Characterisation of cancer cell derived EVs in direct assay. Data from different experiments were accumulated where, (a) Lectin-NPs specific to different glycans were used to detect passively coated EVs-isolated from PCa cell lines (DU145, LNCaP, PC3 and VCaP) using direct assay. (b) Integrin expression of passively coated EVs was analysed using nanoparticles coated with antibodies specific to various integrin sub-units. The heatmap depicts the S/B (signal/background) ratio on a log2 scale.

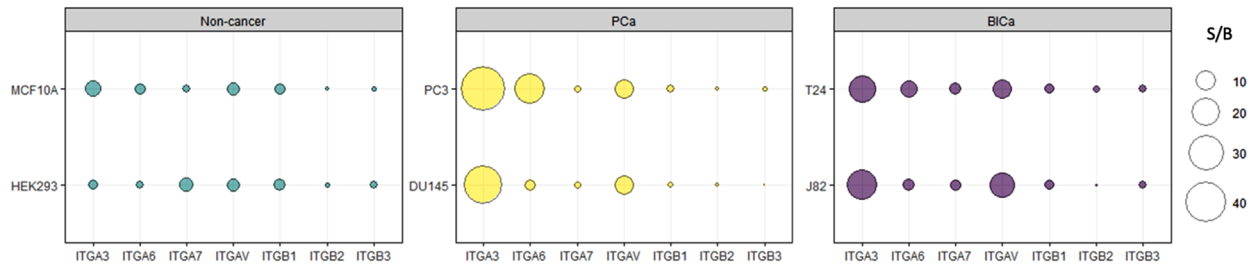

FIGURE 4 Expression of integrins and UEA binding glycans on cell line-derived EVs. Sandwich-assay combining different integrin specific antibodies for capturing of EVs from PCa and BlCa cell lines compared to non-cancer control cell lines. UEA-lectin NPs were used to detect the captured EVs. The size of the bubble constitutes to the S/B ratio obtained from the assay.

and depletion of non-EV enriched proteins such as THP in EV-enriched urine fractions (Figure 5a). Total number and size of particles in EV-enriched and protein-enriched urine fractions were measured by the light scattering method NTA (Figure 5b). Furthermore, urine fractions were assessed by electron microscopy (EM). EM revealed an extensive number of vesicles surrounded by a lipid bilayer within EV-enriched fractions, with an approximate size of 50–200 nm, whereas the protein-enriched fractions show a complex network of protein complexes and polymeric THP (Figure 5c).

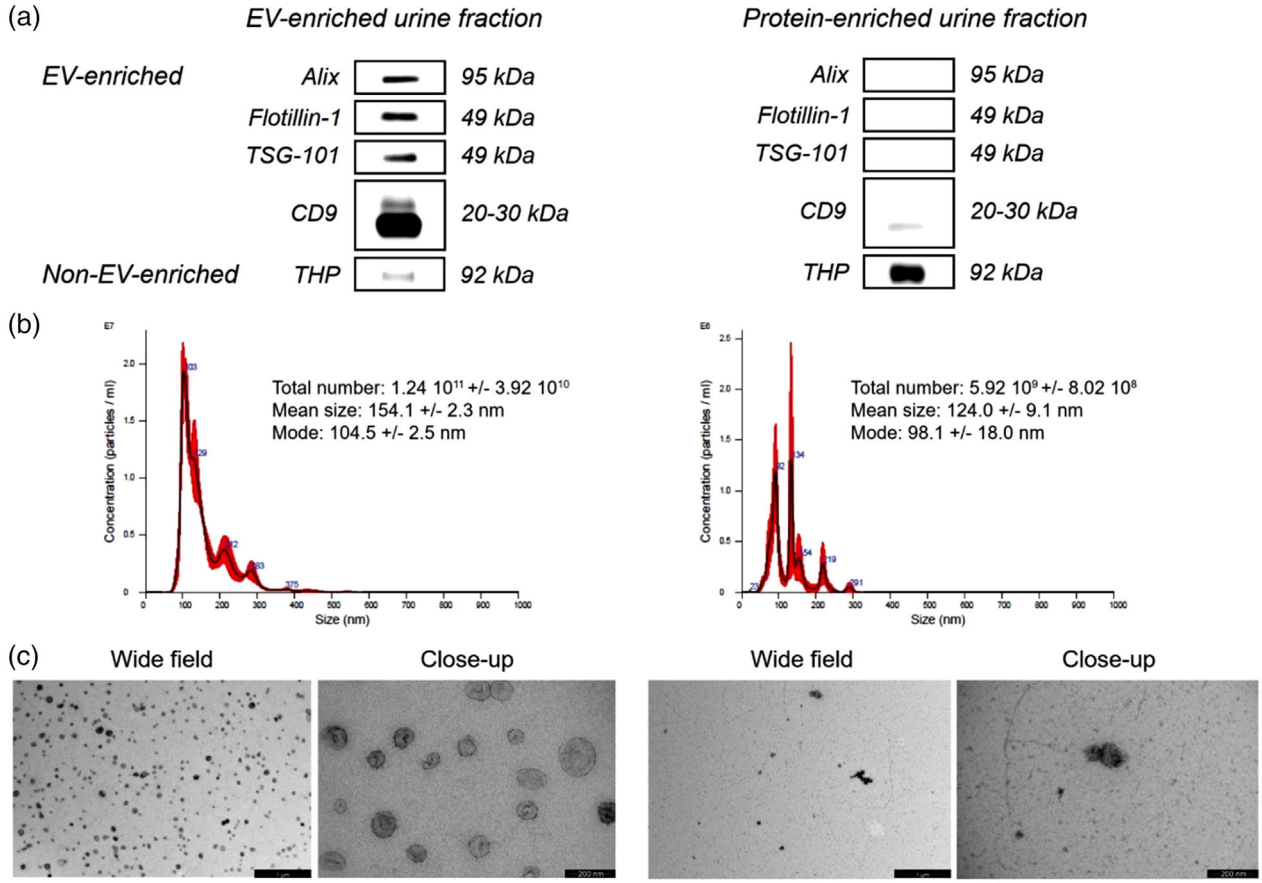

FIGURE 5 Characterisation of EV-enriched and protein-enriched urine preparations. EV-enriched and protein-enriched urine fractions were analysed by (a) WB for Alix, Flotillin-1, TSG-101, CD9 and THP markers (b) NTA for total number of particles and (c) TEM images of vesicle structure and integrity. Here, wide-field (scale bar: 1000 nm) and close-up images (scale bar: 200 nm) are provided.

3.5 | Biomarker characterization from urine derived EVs

To explore the presence of aberrant fucosylation and ITGA3 on EVs in urine, we separated the EV-enriched and protein-enriched (PE) fractions from the urine of five individual BPH, PCa and BlCa patients, using bottom up OptiPrep density gradient centrifugation. Resultant fractions were also assessed for tetraspanins CD63 and CD9, which are known to be enriched on EVs. Both fractions were passively coated on Maxisorp microtiter plates and consecutively detected with nanoparticles (NPs)-coated with either anti-tetraspanin (CD63 & CD9), anti-integrin (ITGA3) antibodies or lectin (UEA). In BPH urine samples, the CD63-, CD9-, ITGA3- and UEA-NP assays showed 2-, 2-, 4- and 66-fold higher S/B ratios in EV-enriched compared to PE fraction, respectively (Figure 6a). In urine of PCa patients, the corresponding values were 46, 3, 3 and 139 for the CD63-, CD9-, ITGA3- and UEA-NP assays, respectively (Figure 6b). Similarly, in urine of BlCa patients, the CD63-, CD9-, ITGA3- and UEA-NP assays exhibited 9-, 4-, 3- and 48-fold higher S/B ratios in EV-enriched fraction than PE fraction, respectively (Figure 6c). Notably, the UEA-NP assays demonstrated the highest S/B ratios in EV-enriched compared to PE fraction derived from urine of BPH, PCa and BlCa samples.

3.6 | Analytical performance of the ITGA3-ITGA3 and glycovariant ITGA3-UEA assays

Performance of the assays were analysed for both the total ITGA3 (ITGA3-ITGA3) and the glycovariant assay utilizing UEA-NP detection (ITGA3-UEA). To assess the linearity and sensitivity (LoD) of both assays, we used purified EVs from DU145 cell line. For ITGA3-ITGA3 assay, the same monoclonal ITGA3 antibody was used both as the capture and the tracer (as coated on NP). Whereas for glycovariant ITGA3-UEA assay, EVs are captured with ITGA3 and detected with lectin UEA that binds to the fucose moieties on EVs and their ITGA3. The limit of detection (LoD) was 2.56×10^8 EVs/ml for the ITGA3-ITGA3 assay and slightly better for the glycovariant assay ITGA3-UEA: 1.38×10^8 EV/ml (Figure 7a).

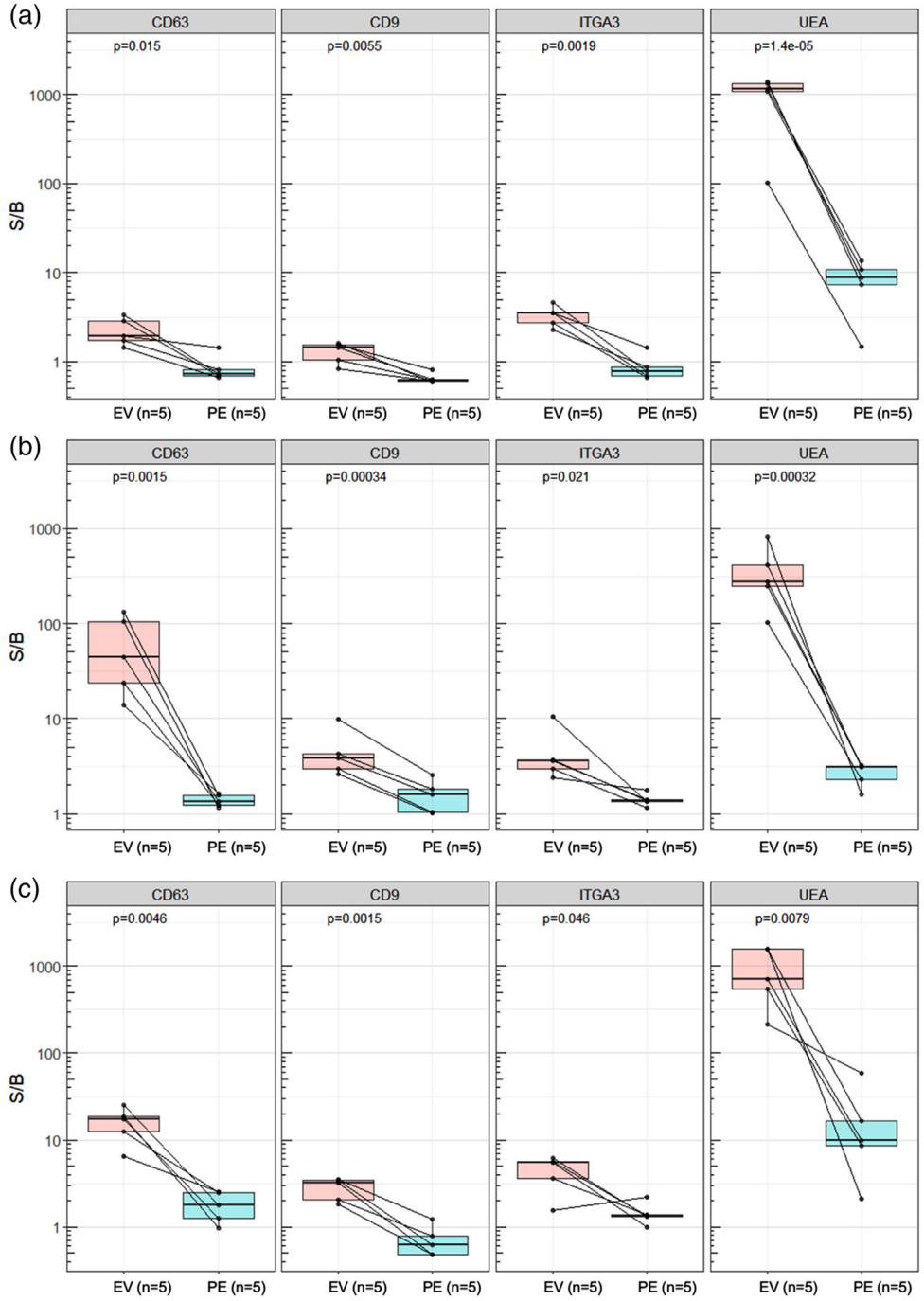

FIGURE 6 Enrichment of biomarkers on urinary EVs. Tetraspanin (CD9 and CD63), integrin (ITGA3) and lectin (UEA) binding to EV and PE fraction isolated from the urine of (a) BPH, (b) PCa and (c) BlCa patients. The x-axis shows EV and PE of individual urine samples used and the y-axis shows the S/B ratios. EV, extracellular vesicles enriched fraction; PE, protein enriched fraction.

3.7 | Clinical performance of the glycovariant ITGA3-UEA assay

Finally, we assessed the clinical performance of the ITGA3-UEA assay by measuring the expression of fucosylated EVs in urine samples from patients with prostate ($n = 32$) and bladder cancer ($n = 32$), compared to urine samples from healthy controls ($n = 18$) and patients with BPH ($n = 30$). The ITGA3-UEA assay showed statistically significant discrimination among patients with BlCa compared to men with BPH (5.5-fold; $p = 0.004$) and PCa (9.2-fold; $p = 0.00038$), as well as healthy individuals (23-fold; $p = 0.0001$) (Figure 7b). In contrast, the ITGA3-UEA assay showed no discrimination between BPH and PCa.

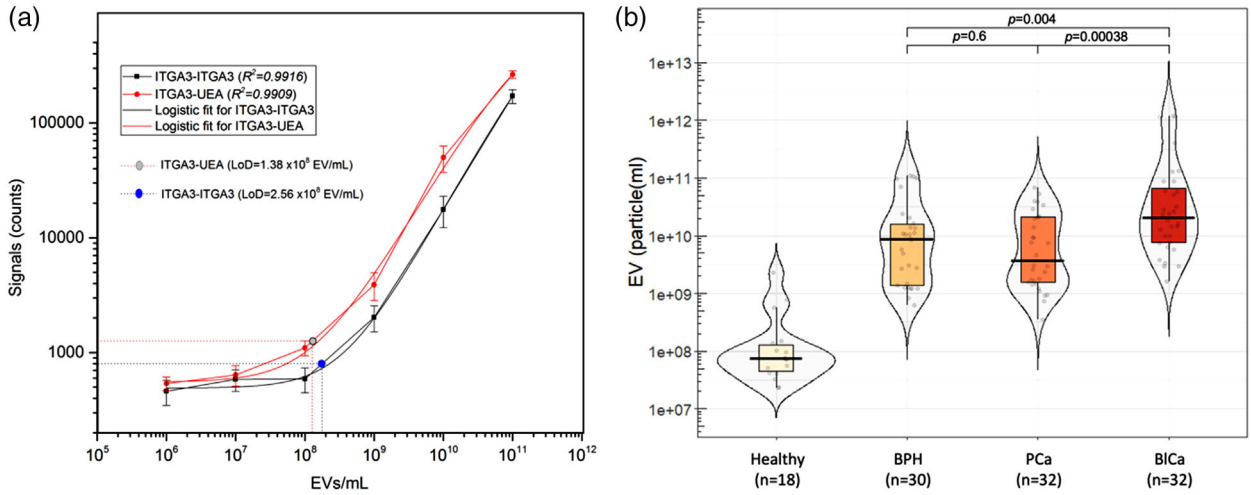

FIGURE 7 (a) Standard curves of ITGA3-ITGA3 and glycovariant ITGA3-UEA assays of DU145-EVs. (b) The performance of ITGA3-UEA assay in detecting uEVs from healthy, BPH, prostate and bladder cancer samples. The ITGA3-UEA assay showed discrimination in BlCa from benign (BPH) source in terms of europium signal counts and *p*-value.

4 | DISCUSSION

Urinary EVs are highly enriched with a myriad of glycosylated proteins, which have shown promise in the detection of urological pathologies (Islam et al., 2021; Jin et al., 2020; Martins et al., 2021). Our findings suggest that a biomarker combination consisting of ITGA3 and fucose is highly expressed on EVs derived from cell line and urine samples. Our results show that by combining a protein-binding antibody with fucose specific lectin in a simple bioaffinity assay, it is possible to detect bladder cancer directly from unprocessed urine.

Previously, Duijvesz and his colleagues demonstrated that same monoclonal tetraspanin specific antibody could capture and detect EVs directly from cell culture medium and urine without the need of extensive preprocessing (Duijvesz et al., 2015). They used europium chelates as a tracer, whereas we have utilized high performance europium-doped polystyrene nanoparticles (Eu^{3+}-NPs) as tracers which are packed with more than 30,000 Eu^{3+} chelates. The antibodies or lectins coated with Eu^{3+}-NPs provide high specific signal activity offering the improved detection sensitivity which are in line with our recently published several bioaffinity assay technologies (Gidwani et al., 2016; Islam et al., 2019; Terävä et al., 2021). However, it is established that lectin-glycan interaction is usually weaker compared to antigen-antibody interaction, the multivalency gained from nanoparticles coating has overcome this problem (Soukka et al., 2001; Syed et al., 2016). Furthermore, in our previous study, we have shown that our developed nanoparticle based TRF approach could detect purified EVs up to 1–13 ng (0.03–0.06 ng/ml) (Islam et al., 2019), whereas Logozzi and his colleagues reported an ELISA based approach that are able to detect EVs up to 3–10 μg (60-200 ng/ml) (Logozzi et al., 2009).

Numerous studies have explored surface glycosylation profiling of uEVs using various lectin-based approaches where purified EVs were prerequisite (Gerlach et al., 2013, 2017; Kosanovic & Jankovic, 2014; Martins et al., 2021). By overcoming the tedious purification process of EVs, our nanoparticles based TRF approach could explore cancer-associated glycosylation patterns on urinary EVs of different urological malignancies. To find out the most abundantly expressed glycans in cancer cell line derived EVs, we profiled four cell lines with 34 lectins manifesting different binding specificities to fucose, galactose, GalNAc, GlcNAc, mannose and sialic acid. As expected, we observed cell line-specific binding patterns for lectins, with exceptionally strong binding with UEA-coated nanoparticles (Figure 3). UEA, a plant lectin isolated from *Ulex europaeus* (gorse) seeds, has affinity to various fucosylated glycan structures, particularly for Fucα1-2Galβ moiety (Du et al., 1994). The results are well in-line with previous studies, which have shown that fucose binding lectins, such as AAL, UEA and TJA-II, might have potential in the detection of PCa (Kekki et al., 2017).

It is known that integrins, and their glycosylation, have a fundamental role in cancer glyco-microenvironment and cancer progression (Marsico et al., 2018). Multiple studies have reported that various integrin (ITG) sub-units including alpha-unit α2, α3, α4, α5, α6, αM, αL, αV and VLA-4 and beta unit β1, β2, β4 and β5 are expressed in urinary EVs and cancer cell lines (Bijnsdorp et al., 2013; Gonzales et al., 2009; Hurwitz & Meckes, 2019; Rieu et al., 2000; Théry et al., 2001; Welton et al., 2010; Wubbolts et al., 2003). Our data confirms previous findings, which suggest that particularly the laminin binding integrins, α3, α6 and to some extent αv are enriched on EVs derived from cancer cell lines (Welton et al., 2010).

In this study, the most abundant integrin ITGA3-based capture was combined with UEA-lectin detection for a sandwich bioaffinity assay. The assay allows detection of cell line derived-EVs with very high signal-to-background ratios (S/B > 10) from

four cancerous cell lines (T24, J82, DU145 and PC3) while manifesting only moderate binding to the control cell lines (MCF10A and HEK293) (Figure 4b). Although the results obtained from individual cell lines never quite translate to clinical samples containing complex mixture of various biomarkers, the high expression of the biomarker combination in all cell lines was a promising starting point for pre-clinical assay development.

To explore the extent of which the biomarker combination is expressed on EVs, we isolated EVs from the urine of three patient sample groups (BPH, PCa and BlCa). As expected, all the previously well-characterized EV-associated markers were significantly enriched on the EV fraction of the isolates (p-value < 0.05). Surprisingly, greatest differences between EV and protein enriched (PE) fractions were observed in the binding of the lectin UEA, particularly in BPH isolates (Figure 5a). This indicated that the glycan structure recognized by UEA evidently is highly enriched to EVs. Defining the exact epitope or antigen to which lectins bind to can be challenging. UEA-I is well known of binding to the Fucα1-2Galβ (h-type 2 antigen) glycan, which is one of the precursors of ABO blood group antigens, although in previous studies ABO-antigens have been excluded from EVs (Williams et al., 2018). Also, the effect of other soluble proteins binding to the EVs, either tethered to THP or unspecifically to the protein corona needs to be studied further. Noteworthy, fucose-binding lectins such as UEA, AAL, PSA, LTA have been reported as diagnostic and prognostic markers in various cancers (Blonski et al., 2007; Dwek et al., 2010; Haselhorst et al., 2001; Kekki et al., 2017; Li et al., 2015; Ohyama et al., 2004).

One of the major gaps in the translation of EV-based biomarkers to the clinic has been the limited availability of analytical standards needed for the development of reproducible and robust assays (Ayers et al., 2019; Erdbrügger et al., 2021). Although significant progress has been made on this front with the introduction of reference materials for EV research (Geeurickx et al., 2021), the biomarkers of interest might not always be expressed on them. To overcome this gap, we used well-characterized EV preparations separated from a commercially available cell line (DU145) to assess the analytical performance of the assay, and also to set up a quantification standard for the clinical urine samples. DU145-derived EVs were selected due to the high expression of the biomarker combination of interest (ITGA3-UEA). Performance wise, both the ITGA3-UEA and ITGA3-ITGA3 assays showed good linearity ($R^2 = 0.991$) and limit-of-detection (1.38×10^8 and 2.56×10^8 particle/ml, respectively) (Figure 7a).

Finally, the established assay was used with individual, unprocessed, urine samples from four patient groups. As expected, all patient groups urological pathologies (BPH, PC and BlCa) were significantly higher in comparison to the healthy donors. Both the mean age of the donors and the number of samples ($n = 18$) likely contribute to the difference. Moreover, the number of EVs and the expression of ITGA3 and fucose on EVs may be associated with age. In a study, Hooten N found that cancer associated proteins increased in EVs with age (Noren Hooten, 2020). Similarly, other studies showed that molecular content as well as number of EVs altered with advanced age (Liang et al., 2017; Yin et al., 2017). The comparison of the patient groups showed a significant elevation of BlCa samples when compared to the PCa and BPH (9.2-fold; $p = 0.00038$ and 5.5-fold; $p = 0.004$, respectively) (Figure 7b). Although the biomarker combination was most prominently found from the cell line material derived from PCa, we did not observe any discrimination between the PCa patient urine samples and controls. Previously we have observed that the expression of ITGA3 is relatively higher in EVs derived from more aggressive prostate cancer PC3 cell line compared to less aggressive LNCaP (Islam et al., 2019). The reason why ITGA3-UEA assay cannot discriminate PCa patients from benign controls might result from the prognostic value of ITGA3 and maybe elevated only in metastatic PCa. Similarly, Bijnsdorp et al. have previously shown that the level of ITGA3 is increased in urinary EVs from metastatic PCa patients compared to non-metastatic PCa (Bijnsdorp et al., 2013). Another significant factor for lower expression can be attributed to sample collection method: the urine samples from PCa patients were collected by catheterization which likely has major impact on the quantity of prostate derived EVs as the urine did not pass the urethra before sampling. Whole urine was collected in biobank urine collection process with clinical laboratory investigations. Where no preprocessing of urine such as centrifugation or filtration was conducted before the storage of sample. Thus, a primary concern with the storage of whole urine samples without any preprocessing is the issue of multiple freezing thawing, with residual cells can be damaged and release intracellular vesicles into the urines (Armstrong et al., 2018). Although it may be a minor percentage of total vesicles population both in cancer and non-cancer cases.

Specificity of ITGA3-ITGA3 and glycovariant ITGA3-UEA assay were determined using pooled urine sample from BPH, PCa and BlCa patients (Figure S2). As expected, we observed that ITGA3-ITGA3 assay shows merely detection of ITGA3 on EVs. Whereas significant discrimination of BlCa from controls is only achieved with glycovariant ITGA3-UEA assay. Thereby, next, we have only run ITGA3-UEA assay with individual clinical samples. Further, to assess the diagnostic value of ITGA3-UEA assay in bladder cancer, area under the curve (AUC = 0.786) was calculated by plotting receiver operating characteristics (ROC) curve (Figure S3).

Eventually this assay platform could potentially be expanded for the detection of other urological cancers by exploring different combinations of integrins and lectins. Although the results are promising particularly for the detection of bladder cancer, this proof of principle assay calls for further clinical and technical evaluation with larger and well-defined patient cohorts in the future. Furthermore, in the follow-up studies, different assay conditions and sample types should be systematically explored, which may increase assay performance (Islam et al., 2019).

5 | CONCLUSIONS

We characterized a novel biomarker combination from urine-derived EVs, which combines ITGA3 capture with lectin nanoparticle detection (ITGA3-UEA). The assay can be used to discriminate BlCa from clinically challenging controls without any preanalytical processing of the samples.

ACKNOWLEDGMENTS

This work is supported by DPMLS-University of Turku graduate school (University of Turku), Academy of Finland (grant no.: 309950/2017), Nanolec project funded by Jane and Aatos Erkko Foundation, MSCA-ITN project proEVLifeCycle (European Union's Horizon 2020 research and innovation programme under grant agreement No 860303) and by InFLAMES Flagship Programme of the Academy of Finland (decision number: 337530). We authors wish to thank Turku Prostate Cancer Consortium (TPCC) for providing clinical samples. The authors also thank Ms. Pauliina Toivonen and PhD student Kimmo Kettunen for collecting clinical samples along with patients' information. We also acknowledge our cancer diagnostics team members for sharing common reagents and outstanding technical assistance.

CONFLICT OF INTEREST

The authors declare that there is no conflict of interest.

REFERENCES

Ahmed, H. U., El-Shater Bosaily, A., Brown, L. C., Gabe, R., Kaplan, R., Parmar, M. K., Collaco-Moraes, Y., Ward, K., Hindley, R. G., Freeman, A., Kirkham, A. P., Oldroyd, R., Parker, C., & Emberton, M. (2017). Diagnostic accuracy of multi-parametric MRI and TRUS biopsy in prostate cancer (PROMIS): A paired validating confirmatory study. *Lancet*, *389*(10071), 815–822.

Andreu, Z., & Yanez-Mo, M. (2014). Tetraspanins in extracellular vesicle formation and function. *Frontiers in Immunology*, *5*, 442.

Armstrong, D. A., Dessaint, J. A., Ringelberg, C. S., Hazlett, H. F., Howard, L., Abdalla, M. A. K., Barnaby, R. L., Stanton, B. A., Cervinski, M. A., & Ashare, A. (2018). Pre-analytical handling conditions and small RNA recovery from urine for miRNA profiling. *The Journal of Molecular Diagnostics*, *20*(5), 565–571.

Ayers, L., Pink, R., Carter, D. R. F., & Nieuwland, R. (2019). Clinical requirements for extracellular vesicle assays. *Journal of Extracellular Vesicles*, *8*(1), 1593755.

Bijnsdorp, I. V., Geldof, A. A., Lavaei, M., Piersma, S. R., van Moorselaar, R. J., & Jimenez, C. R. (2013). Exosomal ITGA3 interferes with non-cancerous prostate cell functions and is increased in urine exosomes of metastatic prostate cancer patients. *Journal of Extracellular Vesicles*, 22097.

Blonski, K., Milde-Langosch, K., Bamberger, A. M., Osterholz, T., Utler, C., Berger, J., Löning, T., & Schumacher, U. (2007). Ulex europeus Agglutinin-I binding as a potential prognostic marker in ovarian cancer. *Anticancer Research*, *27*(4c), 2785–2790.

Charpentier, M., Gutierrez, C., Guillaudeux, T., Verhoest, G., & Pedeux, R. (2021). Noninvasive urine-based tests to diagnose or detect recurrence of bladder cancer. *Cancers (Basel)*, *13*(7), 1650.

Chou, R., Gore, J. L., Buckley, D., Fu, R., Gustafson, K., Griffin, J. C., Grusing, S., & Selph, S. (2015). Urinary biomarkers for diagnosis of bladder cancer: A systematic review and meta-analysis. *Annals of Internal Medicine*, *163*(12), 922–931.

Dhondt, B., Geeurickx, E., Tulkens, J., Van Deun, J., Vergauwen, G., Lippens, L., Miinalainen, I., Rappu, P., Heino, J., Ost, P., Lumen, N., De Wever, O., & Hendrix, A. (2020). Unravelling the proteomic landscape of extracellular vesicles in prostate cancer by density-based fractionation of urine. *Journal of Extracellular Vesicles*, *9*(1), 1736935.

Dhondt, B., Lumen, N., De Wever, O., & Hendrix, A. (2020). Preparation of multi-omics grade extracellular vesicles by density-based fractionation of urine. *STAR Protocols*, *1*(2), 100073.

Du, M. H., Spohr, U., & Lemieux, R. U. (1994). The recognition of three different epitopes for the H-type 2 human blood group determinant by lectins of Ulex europaeus, Galactia tenuiflora and Psophocarpus tetragonolobus (winged bean). *Glycoconjugate Journal*, *11*(5), 443–461.

Dube, D. H., & Bertozzi, C. R. (2005). Glycans in cancer and inflammation–Potential for therapeutics and diagnostics. *Nat Reviews Drug Discovery*, *4*(6), 477–488.

Duijvesz, D., Versluis, C. Y., van der Fels, C. A., Vredenbregt-van den Berg, M. S., Leivo, J., Peltola, M. T., Bangma, C. H., Pettersson, K. S., & Jenster, G. (2015). Immuno-based detection of extracellular vesicles in urine as diagnostic marker for prostate cancer. *International Journal of Cancer*, *137*(12), 2869–2878.

Dwek, M. V., Jenks, A., & Leathem, A. J. (2010). A sensitive assay to measure biomarker glycosylation demonstrates increased fucosylation of prostate specific antigen (PSA) in patients with prostate cancer compared with benign prostatic hyperplasia. *Clinica Chimica Acta*, *411*(23-24), 1935–1939.

Erdbrügger, U., Blijdorp, C. J., Bijnsdorp, I. V., Borràs, F. E., Burger, D., Bussolati, B., Byrd, J. B., Clayton, A., Dear, J. W., Falcón-Pérez, J. M., & Martens-Uzunova, E. S. (2021). Urinary extracellular vesicles: A position paper by the urine task force of the international society for extracellular vesicles. *Journal of Extracellular Vesicles*, *10*(7), e12093.

Fedele, C., Singh, A., Zerlanko, B. J., Iozzo, R. V., & Languino, L. R. (2015). The $\alpha v\beta 6$ integrin is transferred intercellularly via exosomes. *Journal of Biological Chemistry*, *290*(8), 4545–4551.

Ferlay, J., Soerjomataram, I., Dikshit, R., Eser, S., Mathers, C., Rebelo, M., Parkin, D. M., Forman, D., & Bray, F. (2015). Cancer incidence and mortality worldwide: Sources, methods and major patterns in GLOBOCAN 2012. *International Journal of Cancer*, *136*(5), E359–E386.

Geeurickx, E., Lippens, L., Rappu, P., De Geest, B. G., De Wever, O., & Hendrix, A. (2021). Recombinant extracellular vesicles as biological reference material for method development, data normalization and assessment of (pre-)analytical variables. *Nature Protocols*, *16*(2), 603–633.

Gerlach, J. Q., Kruger, A., Gallogly, S., Hanley, S. A., Hogan, M. C., Ward, C. J., Joshi, L., & Griffin, M. D. (2013). Surface glycosylation profiles of urine extracellular vesicles. *Plos One*, *8*(9), e74801.

Gerlach, J. Q., Maguire, C. M., Krüger, A., Joshi, L., Prina-Mello, A., & Griffin, M. D. (2017). Urinary nanovesicles captured by lectins or antibodies demonstrate variations in size and surface glycosylation profile. *Nanomedicine (Lond)*, *12*(11), 1217–1229.

Gidwani, K., Huhtinen, K., Kekki, H., van Vliet, S., Hynninen, J., Koivuviita, N., Perheentupa, A., Poutanen, M., Auranen, A., Grenman, S., Lamminmäki, U., Carpen, O., van Kooyk, Y., & Pettersson, K. (2016). A nanoparticle-lectin immunoassay improves discrimination of serum CA125 from malignant and benign sources. *Clinical Chemistry*, *62*(10), 1390–1400.

Gonzales, P. A., Pisitkun, T., Hoffert, J. D., Tchapyjnikov, D., Star, R. A., Kleta, R., Wang, N. S., & Knepper, M. A. (2009). Large-scale proteomics and phosphoproteomics of urinary exosomes. *Journal of the American Society of Nephrology*, *20*(2), 363–379.

Hamidi, H., & Ivaska, J. (2018). Every step of the way: Integrins in cancer progression and metastasis. *Nature Reviews Cancer*, *18*(9), 533–548.

Harma, H., Soukka, T., & Lovgren, T. (2001). Europium nanoparticles and time-resolved fluorescence for ultrasensitive detection of prostate-specific antigen. *Clinical Chemistry*, *47*(3), 561–568.

Haselhorst, T., Weimar, T., & Peters, T. (2001). Molecular recognition of sialyl Lewis(x) and related saccharides by two lectins. *Journal of the American Chemical Society*, *123*(43), 10705–10714.

Hoshino, A., Costa-Silva, B., Shen, T. L., Rodrigues, G., Hashimoto, A., Tesic Mark, M., Molina, H., Kohsaka, S., Di Giannatale, A., Ceder, S., & Lyden, D. (2015). Tumour exosome integrins determine organotropic metastasis. *Nature*, *527*(7578), 329–335.

Hou, S., Isaji, T., Hang, Q., Im, S., Fukuda, T., & Gu, J. (2016). Distinct effects of β1 integrin on cell proliferation and cellular signaling in MDA-MB-231 breast cancer cells. *Science Reports*, *6*, 18430.

Hurwitz, S. N., & Meckes, D. G., Jr. (2019). Extracellular vesicle integrins distinguish unique cancers. *Proteomes*, *7*(2), 14.

Hurwitz, S. N., Rider, M. A., Bundy, J. L., Liu, X., Singh, R. K., & Meckes, D. G., Jr. (2016). Proteomic profiling of NCI-60 extracellular vesicles uncovers common protein cargo and cancer type-specific biomarkers. *Oncotarget*, *7*(52), 86999–87015.

Huttenlocher, A., & Horwitz, A. R. (2011). Integrins in cell migration. *Cold Spring Harbor Perspectives in Biology*, *3*(9), a005074.

Islam, M. K., Syed, P., Dhondt, B., Gidwani, K., Pettersson, K., Lamminmäki, U., & Leivo, J. (2021). Detection of bladder cancer with aberrantly fucosylated ITGA3. *Analytical Biochemistry*, *628*, 114283.

Islam, M. K., Syed, P., Lehtinen, L., Leivo, J., Gidwani, K., Wittfooth, S., Pettersson, K., & Lamminmäki, U. (2019). A nanoparticle-based approach for the detection of extracellular vesicles. *Science Reports*, *9*(1), 10038.

Jankovic, M. M., & Milutinovic, B. S. (2008). Glycoforms of CA125 antigen as a possible cancer marker. *Cancer Biomark*, *4*(1), 35–42.

Jin, D., Zhang, R., Chen, H., & Li, C. (2020). Aberrantly glycosylated integrin α3β1 is a unique urinary biomarker for the diagnosis of bladder cancer. *Aging (Albany NY)*, *12*(11), 10844–10862.

Kekki, H., Peltola, M., van Vliet, S., Bangma, C., van Kooyk, Y., & Pettersson, K. (2017). Improved cancer specificity in PSA assay using Aleuria aurantia lectin coated Eu-nanoparticles for detection. *Clinical Biochemistry*, *50*(1-2), 54–61.

Kosanovic, M., & Jankovic, M. (2014). Isolation of urinary extracellular vesicles from Tamm- Horsfall protein-depleted urine and their application in the development of a lectin-exosome-binding assay. *Biotechniques*, *57*(3), 143–149.

Lamparski, H. G., Metha-Damani, A., Yao, J. Y., Patel, S., Hsu, D. H., Ruegg, C., & Le Pecq, J. B. (2002). Production and characterization of clinical grade exosomes derived from dendritic cells. *Journal of Immunological Methods*, *270*(2), 211–226.

Li, Q. K., Chen, L., Ao, M. H., Chiu, J. H., Zhang, Z., Zhang, H., & Chan, D. W. (2015). Serum fucosylated prostate-specific antigen (PSA) improves the differentiation of aggressive from non-aggressive prostate cancers. *Theranostics*, *5*(3), 267–276.

Liang, L. G., Kong, M. Q., Zhou, S., Sheng, Y. F., Wang, P., Yu, T., Inci, F., Kuo, W. P., Li, L. J., Demirci, U., & Wang, S. (2017). An integrated double-filtration microfluidic device for isolation, enrichment and quantification of urinary extracellular vesicles for detection of bladder cancer. *Science Reports*, *7*, 46224.

Logozzi, M., De Milito, A., Lugini, L., Borghi, M., Calabro, L., Spada, M., Perdicchio, M., Marino, M. L., Federici, C., Iessi, E., Rivoltini, L., & Fais, S. (2009). High levels of exosomes expressing CD63 and caveolin-1 in plasma of melanoma patients. *Plos One*, *4*(4), e5219.

Lokeshwar, S. D., Ruiz-Cordero, R., Hupe, M. C., Jorda, M., & Soloway, M. S. (2015). Impact of 2004 ISUP/WHO classification on bladder cancer grading. *World Journal of Urology*, *33*(12), 1929–1936.

Lotan, Y., & Roehrborn, C. G. (2003). Sensitivity and specificity of commonly available bladder tumor markers versus cytology: Results of a comprehensive literature review and meta-analyses. *Urology*, *61*(1), 109–118. discussion 118.

Ma, C., Jiang, F., Ma, Y., Wang, J., Li, H., & Zhang, J. (2019). Isolation and detection technologies of extracellular vesicles and application on cancer diagnostic. *Dose Response*, *17*(4), 1559325819891004.

Marsico, G., Russo, L., Quondamatteo, F., & Pandit, A. (2018). Glycosylation and integrin regulation in cancer. *Trends in Cancer*, *4*(8), 537–552.

Martins, Á. M., Ramos, C. C., Freitas, D., & Reis, C. A. (2021). Glycosylation of cancer extracellular vesicles: Capture strategies, functional roles and potential clinical applications. *Cells*, *10*(1), 109.

Mitchell, J. P., Court, J., Mason, M. D., Tabi, Z., & Clayton, A. (2008). Increased exosome production from tumour cell cultures using the integra CELLine culture system. *Journal of Immunological Methods*, *335*(1-2), 98–105.

Noren Hooten, N. (2020). Extracellular vesicles and extracellular RNA in aging and age-related disease. *Translational Medicine of Aging*, *4*, 96–98.

Oeyen, E., Hoekx, L., De Wachter, S., Baldewijns, M., Ameye, F., & Mertens, I. (2019). Bladder cancer diagnosis and follow-up: The current status and possible role of extracellular vesicles. *International Journal of Molecular Sciences*, *20*(4), 821.

Ohyama, C., Hosono, M., Nitta, K., Oh-eda, M., Yoshikawa, K., Habuchi, T., Arai, Y., & Fukuda, M. (2004). Carbohydrate structure and differential binding of prostate specific antigen to maackia amurensis lectin between prostate cancer and benign prostate hypertrophy. *Glycobiology*, *14*(8), 671–679.

Pang, B., Zhu, Y., Ni, J., Thompson, J., Malouf, D., Bucci, J., Graham, P., & Li, Y. (2020). Extracellular vesicles: The next generation of biomarkers for liquid biopsy-based prostate cancer diagnosis. *Theranostics*, *10*(5), 2309–2326.

Paolillo, M., & Schinelli, S. (2017). Integrins and exosomes, a dangerous liaison in cancer progression. *Cancers (Basel)*, *9*(8), 95.

Raitanen, M. P., Leppilahti, M., Tuhkanen, K., Forssel, T., Nylund, P., & Tammela, T. (2001). Routine follow-up cystoscopy in detection of recurrence in patients being monitored for bladder cancer. *Annales Chirurgiae Et Gynaecologiae*, *90*(4), 261–265.

Rana, S., Yue, S., Stadel, D., & Zöller, M. (2012). Toward tailored exosomes: The exosomal tetraspanin web contributes to target cell selection. *International Journal of Biochemistry & Cell Biology*, *44*(9), 1574–1584.

Raposo, G., & Stoorvogel, W. (2013). Extracellular vesicles: Exosomes, microvesicles, and friends. *Journal of Cell Biology*, *200*(4), 373–383.

Rieu, S., Géminard, C., Rabesandratana, H., Sainte-Marie, J., & Vidal, M. (2000). Exosomes released during reticulocyte maturation bind to fibronectin via integrin alpha4beta1. *European Journal of Biochemistry*, *267*(2), 583–590.

Shao, H., Im, H., Castro, C. M., Breakefield, X., Weissleder, R., & Lee, H. (2018). New technologies for analysis of extracellular vesicles. *Chemical Reviews*, *118*(4), 1917–1950.

Shephard, A. P., Giles, P., Mbengue, M., Alraies, A., Spary, L. K., Kynaston, H., Gurney, M. J., Falcón-Pérez, J. M., Royo, F., Tabi, Z., Parthimos, D., Errington, R. J., Clayton, A., & Webber, J. P. (2021). Stroma-derived extracellular vesicle mRNA signatures inform histological nature of prostate cancer. *Journal of Extracellular Vesicles*, *10*(12), e12150.

Siegel, R., Naishadham, D., & Jemal, A. (2013). Cancer statistics, 2013. *CA: A Cancer Journal for Clinicians*, *63*(1), 11–30.

Siegel, R. L., Miller, K. D., & Jemal, A. (2017). Cancer statistics, 2017. *CA: A Cancer Journal for Clinicians*, *67*(1), 7–30.

Siegel, R. L., Miller, K. D., & Jemal, A. (2018). Cancer statistics, 2018. *CA: A Cancer Journal for Clinicians*, *68*(1), 7–30.

Singh, A., Fedele, C., Lu, H., Nevalainen, M. T., Keen, J. H., & Languino, L. R. (2016). Exosome-mediated transfer of αvβ3 integrin from tumorigenic to nontumorigenic cells promotes a migratory phenotype. *Molecular Cancer Research*, *14*(11), 1136–1146.

Smith, Z. L., & Guzzo, T. J. (2013). Urinary markers for bladder cancer. *F1000Prime Reports*, *5*, 21.
Soukka, T., Harma, H., Paukkunen, J., & Lovgren, T. (2001). Utilization of kinetically enhanced monovalent binding affinity by immunoassays based on multivalent nanoparticle-antibody bioconjugates. *Analytical Chemistry*, *73*(10), 2254–2260.
Syed, P., Gidwani, K., Kekki, H., Leivo, J., Pettersson, K., & Lamminmaki, U. (2016). Role of lectin microarrays in cancer diagnosis. *Proteomics*, *16*(8), 1257–1265.
Terävä, J., Tiainen, L., Lamminmäki, U., Kellokumpu-Lehtinen, P. L., Pettersson, K., & Gidwani, K. (2019). Lectin nanoparticle assays for detecting breast cancer-associated glycovariants of cancer antigen 15-3 (CA15-3) in human plasma. *Plos One*, *14*(7), e0219480.
Terävä, J., Verhassel, A., Botti, O., Islam, M. K., Leivo, J., Wittfooth, S., Härkönen, P., Pettersson, K., & Gidwani, K. (2021). Primary breast cancer biomarkers based on glycosylation and extracellular vesicles detected from human serum. *Cancer Report (Hoboken)*, *5*, e1540.
Théry, C., Amigorena, S., Raposo, G., & Clayton, A. (2006). Isolation and characterization of exosomes from cell culture supernatants and biological fluids. *Current Protocols in Cell Biology*, *30*(2), 3–22.
Théry, C., Boussac, M., Véron, P., Ricciardi-Castagnoli, P., Raposo, G., Garin, J., & Amigorena, S. (2001). Proteomic analysis of dendritic cell-derived exosomes: A secreted subcellular compartment distinct from apoptotic vesicles. *Journal of Immunology*, *166*(12), 7309–7318.
Turner, G. A. (1992). N-glycosylation of serum proteins in disease and its investigation using lectins. *Clinica Chimica Acta*, *208*(3), 149–171.
Van Deun, J., Mestdagh, P., Agostinis, P., Akay, Ö., Anand, S., Anckaert, J., Martinez, Z. A., Baetens, T., Beghein, E., Bertier, L., & Hendrix, A. (2017). EV-TRACK: Transparent reporting and centralizing knowledge in extracellular vesicle research. *Nature Methods*, *14*(3), 228–232.
Webber, J., & Clayton, A. (2013). How pure are your vesicles? *Journal of Extracellular Vesicles*, *2*, 19861.
Welton, J. L., Brennan, P., Gurney, M., Webber, J. P., Spary, L. K., Carton, D. G., Falcon-Perez, J. M., Walton, S. P., Mason, M. D., Tabi, Z., & Clayton, A. (2016). Proteomics analysis of vesicles isolated from plasma and urine of prostate cancer patients using a multiplex, aptamer-based protein array. *Journal of Extracellular Vesicles*, *5*, 31209.
Welton, J. L., Khanna, S., Giles, P. J., Brennan, P., Brewis, I. A., Staffurth, J., Mason, M. D., & Clayton, A. (2010). Proteomics analysis of bladder cancer exosomes. *Molecular & Cellular Proteomics*, *9*(6), 1324–1338.
Williams, C., Royo, F., Aizpurua-Olaizola, O., Pazos, R., Boons, G. J., Reichardt, N. C., & Falcon-Perez, J. M. (2018). Glycosylation of extracellular vesicles: Current knowledge, tools and clinical perspectives. *Journal of Extracellular Vesicles*, *7*(1), 1442985.
Wubbolts, R., Leckie, R. S., Veenhuizen, P. T., Schwarzmann, G., Möbius, W., Hoernschemeyer, J., Slot, J. W., Geuze, H. J., & Stoorvogel, W. (2003). Proteomic and biochemical analyses of human B cell-derived exosomes. Potential implications for their function and multivesicular body formation. *Journal of Biological Chemistry*, *278*(13), 10963–10972.
Yin, Y., Chen, H., Wang, Y., Zhang, L., & Wang, X. (2017). Roles of extracellular vesicles in the aging microenvironment and age-related diseases. *Journal of Extracellular Vesicles*, *10*(12), e12154.
Zhang, Y., Liu, Y., Liu, H., & Tang, W. H. (2019). Exosomes: Biogenesis, biologic function and clinical potential. *Cell & Bioscience*, *9*, 19.
Zhou, B., Xu, K., Zheng, X., Chen, T., Wang, J., Song, Y., Shao, Y., & Zheng, S. (2020). Application of exosomes as liquid biopsy in clinical diagnosis. *Signal Transduction Target Therapy*, *5*(1), 144.

SUPPORTING INFORMATION

Additional supporting information can be found online in the Supporting Information section at the end of this article.

How to cite this article: Islam, M. K., Dhondt, B., Syed, P., Khan, M., Gidwani, K., Webber, J., Hendrix, A., Jenster, G., Lamminen, T., Boström, P. J., Pettersson, K., Lamminmäki, U., & Leivo, J. (2022). Integrins are enriched on aberrantly fucosylated tumour-derived urinary extracellular vesicles. *Journal of Extracellular Biology*, *1,* e64.
https://doi.org/10.1002/jex2.64